NeuroImage: Clinical 27 (2020) 102318

Contents lists available at ScienceDirect

NeuroImage: Clinical

journal homepage: www.elsevier.com/locate/ynicl

Beyond the eye: Cortical differences in primary visual processing in children with cerebral palsy

Jacy R. VerMaas[a,b], Christine M. Embury[b,c,d,e], Rashelle M. Hoffman[a,b], Michael P. Trevarrow[a,b,e], Tony W. Wilson[b,d,e], Max J. Kurz[a,b,e,*]

[a] Department of Physical Therapy, Munroe-Meyer Institute, University of Nebraska Medical Center, Omaha, Nebraska
[b] Center for Magnetoencephalography, College of Medicine, University of Nebraska Medical Center, Omaha, Nebraska
[c] Department of Psychology, University of Nebraska – Omaha, Nebraska
[d] Department of Neurological Sciences, University of Nebraska Medical Center, Omaha, Nebraska
[e] Cognitive Neuroscience of Development & Aging (CoNDA) Center, University of Nebraska Medical Center, Omaha, NE, USA

ARTICLE INFO

Keywords:
Magnetoencephalography
MEG
Vision
Visual perception
Contrast
Spatial gratings

ABSTRACT

Despite the growing clinical recognition of visual impairments among people with cerebral palsy (CP), very few studies have evaluated the neurophysiology of the visual circuitry. To this end, the primary aim of this investigation was to use magnetoencephalography and beamforming methods to image the relative change in the alpha–beta and gamma occipital cortical oscillations induced by a spatial grating stimulus (*e.g.*, visual contrast) that was viewed by a cohort of children with CP and typically-developing (TD) children. Our results showed that the high-contrast, visual gratings stimuli induced a decrease in alpha–beta (10 – 20 Hz) activity, and an increase in both low (40 – 56 Hz) and high (60 – 72 Hz) gamma oscillations in the occipital cortices. Compared with the TD children, the strength of the frequency specific cortical oscillations were significantly weaker in the children with CP, suggesting that they had deficient processing of the contrast stimulus. Although CP is largely perceived as a musculoskeletal centric disorder, our results fuel the growing impression that there may also be prominent visual processing deficiencies. These visual processing deficits likely impact the ability to perceive visual changes in the environment.

1. Introduction

Cerebral palsy (CP) is a prevalent neurodevelopmental disorder in which early brain damage results in neuromuscular impairments and sensory-perceptual disturbances (Rosenbaum et al., 2007). While the literature on CP primarily focuses on the sensorimotor impairments, a relatively small body of literature has examined visual dysfunction in children with CP. Despite the paucity of studies, visual dysfunction is now recognized as a core, co-occurring disorder affecting between 50% and 90% of those with CP (Ego et al., 2015; Fazzi et al., 2007, 2012; Pueyo et al., 2009). Visual function is especially important as precise visual information is crucial for understanding our environment and making accurate motor decisions (Krigolson et al., 2015). When the visual system is unable to efficiently process low-level visual information, all other visual computations and processes reliant on this information may be disturbed (Perreault et al., 2015), potentially contributing to diminished motor performance in everyday activities (Deramore Denver et al., 2016; Salavati et al., 2014).

Several studies have reported that children with CP may have ocular abnormalities such as refractive errors, optic atrophy and optic disc pallor (da Cunha Matta et al., 2008; Fazzi et al., 2012; Ghate et al., 2016; Kozeis et al., 2015; Park et al., 2016). In addition, these children may have oculomotor impairments resulting in difficulty with fixation, smooth pursuits, saccadic movements or strabismus (Kozeis et al., 2015, 2007; da Cunha Matta et al., 2008; Fazzi et al., 2012). Clinical reports also indicate that there may be a high incidence of more nuanced brain-based visual dysfunctions in those with CP, including basic visual perception deficits (*e.g.*, contrast sensitivity, acuity) and higher-level visual disorders involving perception and integration (*e.g.*, visual-cognitive disorders; Fazzi et al., 2012; Kozeis et al., 2015; Schmetz et al., 2018; Stiers et al., 2002). Given the high prevalence of such visual aberrations in those with CP, it appears likely that the perinatal brain insults that underlie the characteristic sensorimotor impairments seen in CP concurrently affect aspects of the visual processing pathway (*e.g.*,

* Correpsonding author: Department of Physical Therapy, Munroe-Meyer Institute for Genetics and Rehabilitation, University of Nebraska Medical Center, 985450 Nebraska Medical Center, Omaha, Nebraska 68198-5450.
E-mail address: mkurz@unmc.edu (M.J. Kurz).

https://doi.org/10.1016/j.nicl.2020.102318
Received 7 January 2020; Received in revised form 3 June 2020; Accepted 16 June 2020
Available online 19 June 2020

geniculostriate, optic radiations, visual cortex; Chokron & Dutton, 2016; Dutton et al., 2006; Fazzi et al., 2012). Consequently, there is likely a strong connection between the motor presentations seen in those with CP and the degree of the visual processing impairments.

The processing of contrast is a low-level visual processing component that develops early in life and occurs early in the visual processing stream (Braddick & Atkinson, 2011). Adequate processing of visual contrast allows one to determine the edge of a step or discriminate a rock from the background of the sidewalk. Additionally, contrast gratings may be used to determine visual acuity, another fundamental aspect of vision (Braddick & Atkinson, 2011). Several magnetoencephalographic (MEG) brain imaging studies have shown that viewing sinusoidal gratings with high contrast elicits a oscillatory response consisting of a sustained increase in gamma (> 30 Hz) activity in the primary visual (V1) cortices, as well as a decrease in the strength of alpha and beta (8 – 25 Hz) activity in more lateral occipital cortices (Adjamian et al., 2004; Hall et al., 2005; Swettenham, Muthukumaraswamy, & Singh, 2009). These spectrally-specific neural responses may serve different visual processes. The strength of the gamma response is dependent upon the contrast properties of the stimulus, while the strength of the alpha–beta power decrease is not contrast dependent (Swettenham et al., 2009). Magnetic resonance spectroscopy (MRS) suggests that individual differences in visual gamma power are likely dependent upon local γ-Aminobutyric acid (GABA) inhibitory interneuronal connections to pyramidal cells (Muthukumaraswamy & Singh, 2009). Furthermore, structural imaging has suggested that the thickness of local gray matter within visual cortices is closely related to the strength of occipital gamma oscillatory activity (Muthukumaraswamy et al., 2010). As for the alpha–beta oscillations, the consensuses is that they are central to visual processing and the engagement of visual attention (Ikkai, Dandekar, & Curtis, 2016). These responses are generally centered in more lateral occipital visual cortices, bilaterally, and are seen during the processing of almost all visual input (Adjamian et al., 2004; Braddick & Atkinson, 2011; Hall et al., 2005; Swettenham et al., 2009). Although we currently have in depth knowledge about the cortical oscillations associated with visual processing in healthy controls, no studies to date have determined if such cortical oscillations are altered in children with CP during processing of high-contrast stimuli. Such information will provide key data on the neurophysiological underpinnings of the more nuanced visual processing deficits noted in the clinic for these children. In addition, these data will aide in the development of more precise therapeutic treatments that target the specific neuro-physiological processes that are contributing to the visual deficits.

To date, our MEG investigations have begun to evaluate the potential alterations in cortical visual function seen in children with CP. We initially identified that children with CP have weaker cortical oscillations in the primary visual cortices (V1) while performing a visuomotor knee isometric force production task (Kurz et al., 2017). Given that the task in Kurz et al. (2017) involved components of stimulus tracking, we conducted a follow-up investigation that isolated the cortical oscillations associated with visual motion in the V5/Visual MT cortical area by having children track a series of moving dots (VerMaas et al., 2019). These results showed that the children with CP had weaker alpha–beta (8 – 20 Hz) cortical oscillations in the V5/Visual MT area during visual motion, implying that visual processing deficits in CP extend beyond the primary visual cortices (VerMaas et al., 2019). Despite the clinical inferences taken away from these investigations, we still have a limited understanding of the neurophysiology underlying most aspects of visual stimulus processing in children with CP. Obviously, the identification of contrasting stimuli plays a prominent role in our visual perception and acuity. Therefore, the primary aim of this investigation was to quantify the strength of visual cortical oscillations induced by a static high-contrast spatial gratings image in children with CP and typically-developing (TD) children. Our systematic evaluation of sub-components of the visual processing networks in children with CP is directed at enhancing the identification and treatment of specific visual problems that may be impacting how children with CP perceive environmental change.

Table 1
Demographics of the participating children with spastic cerebral palsy (CP). GMFCS = Gross Motor Function Classification Score. Children with a level I walk independently, level II walk with some limitations, level III primarily use crutches or a walker while walking, and level IV primarily use power mobility.

Child with CP	Age (years)	Sex	GMFCS Level	CP subtype
1	16.7	F	I	Diplegia
2	16.7	M	III	Diplegia
3	11.6	M	II	Right Hemiplegia
4	15.4	F	III	Diplegia
5	11.0	F	II	Diplegia
6	14.9	F	III	Diplegia
7	16.8	M	II	Diplegia
8	11.5	M	I	Diplegia
9	15.8	M	I	Diplegia
10	13.8	F	I	Diplegia
11	10.6	F	II	Right Hemiplegia
12	9.3	F	I	Right Hemiplegia
13	11.8	F	II	Diplegia
14	17.8	M	III	Diplegia
15	11.3	F	III	Diplegia
16	10.7	M	II	Right Hemiplegia
17	10.1	M	II	Left Hemiplegia
18	12.0	M	I	Left Hemiplegia
19	13.4	F	IV	Diplegia
20	12.3	F	II	Right Hemiplegia
21	18.9	M	II	Diplegia

2. Materials and methods

2.1. Participants

A total of 46 children participated in this investigation. In this study, the term “children” is defined as anyone under 18 years-old at the time of enrollment. Twenty-one children had been diagnosed with CP (age = 13.4 ± 2.8 yrs.; 12 females) and twenty-five were TD (age = 14.5 ± 3.1 yrs.; 11 females). Visual inspection of the MR images of the participants showed no visible signs of atrophy or damage to the occipital cortices. All participants were free of metal implants that could interfere with the MEG or be a MRI safety hazard. The TD participants had no known visual, neurological, developmental, or musculoskeletal impairments. The demographics of the children with CP are shown in Table 1. The children with CP that participated in this study were referred from the staff occupational and physical therapists at the Munroe-Meyer Institute who provide educational services in the school setting. As part of their educational services, all of the children undergo a vision screening to determine if they have visual deficits that need to be addressed. This visual screening includes near (40.6 cm) and far (6 m) distance visual acuity in right/left eye, and pass/fail tests for amblyopia, strabismus, and internal/external eye health. The children that were referred for this study were listed as having normal or corrected to normal visual acuity when using both eyes and could focus at a distance of 1 m. None of the participants were identified as having challenges with functional vision that impacted their activities of daily living or access to educational materials. All of the parents provided written consent that their child could participate in the investigation, and the children assented. The Institutional Review Board at the University of Nebraska Medical Center reviewed and approved the protocol for this investigation.

2.2. MEG data acquisition and experimental paradigm

Neuromagnetic responses were sampled continuously at 1 kHz with an acquisition bandwidth of 0.1 – 330 Hz using an Elekta MEG system

(Helsinki, Finland) with 306 magnetic sensors, including 204 planar gradiometers and 102 magnetometers. All recordings were conducted in a one-layer magnetically-shielded room with active shielding engaged for advanced environmental noise compensation. For the experiment, the participants were seated upright in a magnetically silent chair with their head positioned within the helmet-shaped MEG sensor array. A custom-built head stabilization device that consisted of a series of inflatable airbags that surrounded the sides of the head and filled the void between the head and MEG helmet was worn during the data collection in order to stabilize the head and reduced the probability of any large head movements. To assess the neural processing of primary visual information, the participant viewed a series of vertical, stationary, square wave gratings (3 cycles per degree) that have been previously shown to evoke robust power changes in the alpha (8 – 16 Hz range) and gamma (40 – 56 Hz range) bands (Adjamian et al., 2004; Hall et al., 2005; Swettenham et al., 2009; Wilson et al., 2017). Images were displayed on a back-projected flat screen at eye-level and approximately one meter away. The participants were instructed to fixate on a central red square that remained present throughout the paradigm. Each visual presentation trial began with the appearance of the stationary gratings that remained visible for 500 ms before disappearing. The inter-stimulus interval varied between 2.2 and 2.6 s, and 120 visual stimulations were presented (Fig. 1).

2.3. MEG coregistration

For the MEG experiment, four coils were affixed to the head of each participant and were used for continuous head localization. Prior to the experiment, the location of these coils, three fiducial points, and the scalp surface was digitized to determine their three-dimensional position (Fastrak 3SF0002, Polhemus Navigator Sciences, Colchester, VT, USA). During the MEG recording, an electric current with a unique frequency label (*e.g.*, 322 Hz) was fed to each of the four coils. This induced a measurable magnetic field and allowed each coil to be localized throughout the recording session. Since the coil locations were also known in head coordinates, all MEG measurements could be transformed into a common coordinate system. With this coordinate system (including the scalp surface points), each participant's MEG data was coregistered with their neuro-anatomical MRI data using the three external landmarks (*i.e.*, fiducials) and the digitized scalp surface points prior to source space analyses. The neuroanatomical MRI data were aligned parallel to the anterior and posterior commissures and transformed into standardized space using BESA MRI (Version 2.0; BESA GmbH, Gräfelfing, Germany).

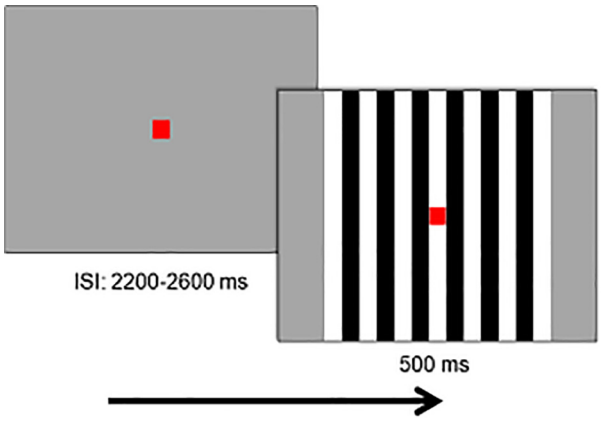

Fig. 1. MEG visual task. Participants were positioned upright one meter from the stimulus screen and maintained visual fixation on the central red square throughout the task. A static spatial-grating stimulus was presented for 500 ms, with an interstimulus interval (ISI) of 2200–2600 ms. Each participant viewed 120 spatial-grating trials during the experiment. (For interpretation of the references to color in this figure legend, the reader is referred to the web version of this article.)

2.4. MEG pre-processing & time-frequency transformation

Using the MaxFilter software (Elekta), each MEG dataset was individually corrected for head motion that may have occurred during the visual processing experiment and was subjected to noise reduction using the signal space separation method with a temporal extension (Taulu & Simola, 2006). Cardiac and blink artifacts were removed from the data using signal-space projection (SSP), which was accounted for during source reconstruction (Uusitalo & Ilmoniemi, 1997). The continuous magnetic time series was divided into epochs of 1300 ms in duration (-400 ms to + 900 ms; time 0 ms defined as the onset of the first visual grating), with the baseline period defined as -350 to -50 ms. Artifact rejection was performed using a fixed threshold method and supplemented with visual inspection. This quality check resulted in four of the participants (CP = 1, TD = 3) being excluded due to notable MEG artifacts. The epoch acceptance rate was 82% (98 ± 4 epochs) for the remaining participants, with no statistical difference in acceptance rate between groups ($p = 0.86$).

The artifact-free epochs were transformed into the time–frequency domain using complex demodulation (Kovach & Gander, 2016), and the resulting spectral power estimations per sensor were averaged over trials to generate time–frequency plots of the mean spectral density. These sensor-level data were normalized using the respective bin's baseline power (-350 ms to -50 ms time window). The specific time–-frequency windows used for imaging were determined by a fully data-driven approach that began with a statistical analysis of the sensor-level spectrograms across the entire array of gradiometers across all participants. Each data point in the spectrogram was initially evaluated using a mass-univariate approach based on the general linear model. To reduce the risk of false positive results while maintaining reasonable sensitivity, a two-stage procedure was followed to control for Type 1 error. In the first stage, paired-sample t-tests (baseline vs. visual presentation) were conducted on each data point, and the output spectrogram of t-values was thresholded at $p < 0.05$ to define time–-frequency bins containing potentially significant oscillatory deviations across all participants. In stage two, time–frequency bins that survived the threshold were clustered with temporally and spectrally neighboring bins that were also above the threshold ($p < 0.05$), and a cluster value was derived by summing all of the *t*-values of all data points in the cluster. Nonparametric permutation testing was then used to derive a distribution of cluster-values, and the significance level of the observed clusters (from stage one) were tested directly using this distribution (Maris & Oostenveld, 2007). For each comparison, at least 1,000 permutations were computed to build a distribution of cluster values. Based on these analyses, the time–frequency windows that contained significant oscillatory events across all participants (described in the Results section) were subjected to a beamforming analysis.

2.5. MEG source imaging & statistics

A minimum variance vector beamforming algorithm was employed to calculate the source power across the entire brain volume (Gross et al., 2001; Hillebrand et al., 2005). The single images were derived from the cross-spectral densities of all combinations of MEG sensors, and the solution of the forward problem for each location on a grid specified by input voxel space. Following convention, the source power in these images was normalized per subject using a separately averaged pre-stimulus noise period of equal duration and bandwidth (Hillebrand et al., 2005; Van Veen et al., 1997). Such images are typically referred to as pseudo-t maps, with units (pseudo-t) that reflect noise-normalized power differences (*i.e.*, visual presentation vs. baseline) per voxel. The resulting beamformer images were 4.0 × 4.0 × 4.0 resolution and

were transformed into standard space by using the transform that was previously applied to the structural MRI volume and then spatially re-sampled. MEG pre-processing and imaging was performed with the Brain Electrical Source Analysis software (BESA v6.0; Grafelfing, Germany).

We imaged the statistically-defined time–frequency windows in each participant using a beamformer and then averaged all output pseudo-t maps across participants to identify the peak voxels, which were used to identify group differences in the cortical oscillations of interest. To examine the dynamics, the virtual sensor (*i.e.*, voxel time series) for the peak voxel per response were computed by applying the sensor-weighting matrix derived through the forward computation to the preprocessed signal vector, which yielded a time series for each source vector centered in the voxel of interest (Cheyne et al., 2006; Heinrichs-Graham et al., 2016; Heinrichs-Graham & Wilson, 2016). An average of the respective time courses was subsequently created to qualitatively evaluate the changes seen in each frequency band of interest.

3. Results

3.1. Sensor space analysis

Presentation of the visual stimulus was associated with strong oscillatory power changes across a large number of gradiometers over the occipital cortices (Fig. 2). These grand-averaged sensor-level spectrograms showed a robust increase in power that began 50 ms after the visual stimulus and stretched across a broad frequency band (20 – 72 Hz), and was sustained in the high-gamma (60 – 72 Hz) frequency range for about 300 ms. Statistical analyses revealed separate components of increased power within the beta (20 – 36 Hz, 50 – 100 ms), low-gamma (40 – 56 Hz, 50 – 100 ms), and high-gamma (60 – 72 Hz, 50 – 350 ms) frequency ranges ($p < 0.001$, corrected; Fig. 2). Concurrently, a significant decrease in the power was detected in the alpha–beta (10 – 20 Hz) frequency range during the 175 to 475 ms time window ($p < 0.001$, corrected; Fig. 2). To identify the brain regions generating these oscillatory responses, we beamformed each of these respective time–frequency windows.

3.2. Alpha and beta cortical oscillations

The beamformer images for the power increase seen in the beta (20 – 36 Hz) band during the 50 – 100 ms time window (baseline = -100 to -50 ms) revealed activity bilaterally in the occipital cortices. The individual pseudo-t values from the peak voxels of the respective hemispheres were subsequently extracted for each participant and averaged, as we did not have hemisphere-specific hypotheses. Group-wise statistical testing indicated that the strength of the beta increase did not differ between groups (TD = 4.2 ± 1.3; CP = 2.9 ± 0.7; $p = 0.36$).

The beamforming images for the decrease in alpha–beta (10 – 20 Hz) power during the latter 175 – 475 ms time window (baseline = -350 to -50 ms) indicated that these neural oscillatory responses extended across the occipital cortices (Fig. 3). The pseudo-t value from the peak voxel in each hemisphere was extracted and averaged per participant, as again we had no hemisphere-specific hypotheses. Group-wise statistics indicated that the strength of the alpha–beta decrease seen in the occipital cortices was significantly stronger for the TD group compared to the group with CP ($p < 0.001$). To determine the temporal dynamics, we extracted the neural time course from the peak voxel from each hemisphere and averaged the respective time courses. These time courses showed that the strength of the alpha–beta decreases were stronger for the TD group beginning at 75 ms and continued to be stronger throughout the presentation of the visual stimulus.

Lastly, to inform future studies, we performed an exploratory analysis by dividing groups based on type of CP (hemiplegic and diplegic) and GMFCS level to examine a potential relationship with the strength of the cortical oscillations. The strength of the beta response did not differ between children with hemiplegia and diplegia forms of CP ($p = 0.96$) or by GMFCS levels ($p = 0.40$).

3.3. Gamma cortical oscillations

The low-gamma (40 – 56 Hz) during the 50 to 100 ms time window (baseline -100 to -50 ms; Fig. 4) and high-gamma (60 – 72 Hz) oscillations during the 50 to 350 ms time window (baseline -350 to -50 ms; Fig. 5) were generated by the occipital cortices bilaterally. The pseudo-*t* values from the peak voxels of the respective frequency bands were subsequently extracted and averaged across hemispheres per response. The results indicated that the stimulus induced a significantly weaker gamma responses in both the low ($p = 0.01$) and high-gamma range ($p = 0.01$) in those with CP compared to the TD children. The neural time courses from the peak voxels were subsequently extracted to evaluate these differences. These time courses showed that the children with CP had notably weaker low and high-gamma oscillations compared with the TD children throughout the stimulus duration.

Analogous to our approach for alpha and beta oscillations, the children with CP were further divided into groups based on type of CP (hemiplegic and diplegic) and GMFCS level to examine a potential relationship with the strength of the low- and high-gamma cortical oscillations. The strength of both gamma responses did not differ between children with hemiplegia and diplegia forms of CP (low-gamma, $p = 0.34$; high-gamma, $p = 0.44$) or by GMFCS levels (low-gamma, $p = 0.30$; high-gamma, $p = 0.86$).

4. Discussion

A number of studies have begun to establish visual processing impairments in children with CP using behavioral-observational methodologies (Ego et al., 2015; Fazzi et al., 2007, 2012; Pueyo et al., 2009). Yet, the neural mechanisms that underlie these deficits remain, for the

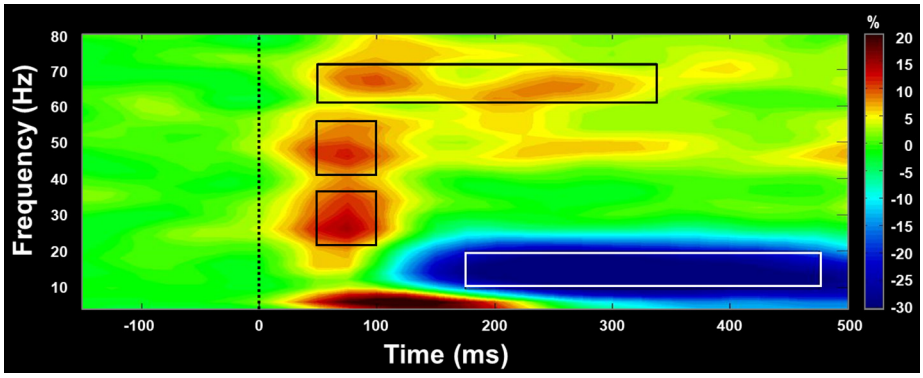

Fig. 2. Time-frequency spectrogram from a gradiometer sensor located over the occipital cortex averaged across all participants. Time (in ms) is denoted on the *x*-axis, with 0 ms defined as the onset of the spatial grating. Spectral power is expressed as the difference from the baseline period (-350 to -50 ms). Separate components of significantly increased power were seen across the beta (20–36 Hz, 50 – 100 ms), low-gamma (40 – 56 Hz, 50 – 100 ms) and high-gamma (60 – 72 Hz, 50 – 350 ms) frequency bands. In addition, there was a significant decrease in power in the alpha–beta (10 – 20 Hz) frequency band during the latter time window (175 to 475 ms). Permutation testing indicated that all components were significant relative to baseline, $p < 0.001$, corrected.

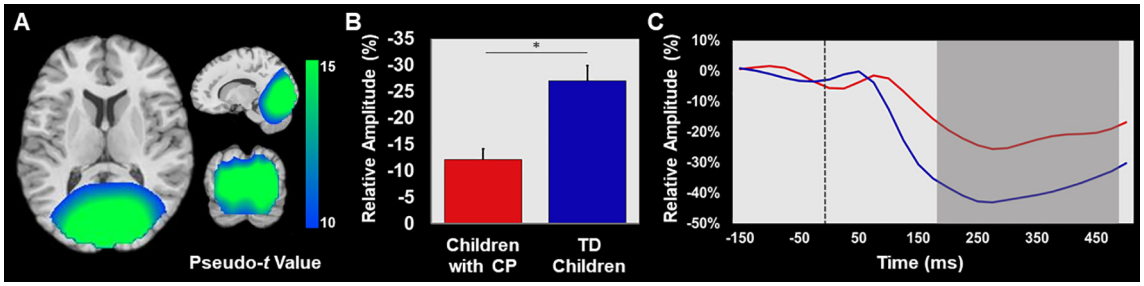

Fig. 3. Alpha-beta (10 – 20 Hz) occipital cortical oscillations during the 175 to 475 ms time window. A) The grand-averaged beamformer image shows that the alpha–beta oscillations were centered on the occipital cortices. The pseudo-*t* color bar is shown to the right of the image. B) Relative response values (pseudo-*t*) averaged across participants per group, with * indicating $p < 0.001$. C) The neural time course was extracted from the peak voxel of each hemisphere, and then averaged across hemispheres for each group. The time series of the children with CP are plotted in red, while the TD participants are plotted in blue. Time (ms) is denoted on the *x*-axis with relative amplitude (%) shown on the *y*-axis. The visual stimulus was presented at 0 ms (dotted line), and the time–frequency window imaged is shown in the grayed area. The TD group demonstrated a stronger decrease in the alpha–beta occipital cortical oscillations throughout the stimulus presentation compared to the group with CP. (For interpretation of the references to color in this figure legend, the reader is referred to the web version of this article.)

most part, completely unknown. This study used MEG and beamforming methods to quantify the occipital cortical oscillations while TD children and children with CP viewed stationary high-contrast stimuli. Our results showed that the induced changes in the strength of the alpha–beta and gamma cortical oscillations were weaker in the children with CP. These results indicate that the altered alpha–beta and gamma cortical oscillations likely play a role in the aberrant visual processing frequently observed clinically. Further discussion of the implication of these results are detailed in the following sections.

Compared with the TD participants, those with CP had weaker gamma oscillatory activity in the occipital cortices while viewing the spatial gratings. Prior research has suggested that such gamma oscillations are linked with bottom up processing of visual information (Bastos et al., 2015; Pelt et al., 2016; Saleem et al., 2017; Takesaki et al., 2016). This may indicate that the initial cortical processing of fine visual features are degraded in those with CP. A previous MRS and PET study has also shown that gamma oscillations are dependent upon the interconnection between the pyramidal cells and GABAergic inhibitory interneurons (Kujala et al., 2015; Muthukumaraswamy & Singh, 2009). This relationship might explain the weaker gamma results presented here since prior PET studies have also shown that participants with CP tend to have increased GABA receptor binding potential within the cortices (Lee et al., 2011; Park et al., 2013). Hence, we suspect that the weaker gamma responses seen in this investigation is to some degree a result of altered GABA activity. Conceptually, aberrant gamma oscillations would result in more downstream errors in the higher-level integration of the incoming visual information.

The children with CP also had weaker decreases in their alpha–beta activity within the occipital cortices while viewing the gratings. Such alpha and beta cortical oscillations have been associated with top-down processing of the visual feedback (Bastos et al., 2015; Kerkoerle et al., 2014), and are thought to influence the neural computations early in the visual stream that are involved in the perception of a visual stimulus (Li et al., 2004; Piech et al., 2013). Hence, it is possible that the perceptual errors seen in children with CP may be related to top-down visual processing. A prior MEG study has also shown that the alpha–-beta oscillations are central to the engagement of visual attention (Ikkai et al., 2016). Hence, it is alternatively feasible that the weaker alpha–beta oscillations seen in the children with CP might be linked with their inability to sustain attention on the visual stimuli.

Despite the high prevalence of visual processing impairments in children with CP recognized in the literature and in the definition of CP, these aberrations continue to be overlooked in the medical and educational communities. Frankly, many of the perinatal brain lesions that cause the characteristic motor impairments in CP are also implicated in the etiology of visual dysfunction (Jacobson et al., 2010). Hence, the visual dysfunction and the motor dysfunction may be intricately linked. For example, individuals with CP may have periventricular leukomalacia, which frequently affects the development of the optic radiations (Hoon et al., 2009). Periventricular leukomalacia has been associated with visual (Fazzi et al., 2009; Lennartsson et al., 2014), as well as motor dysfunction. Additionally, the basal ganglia may contribute to the motor dysfunction in those with CP (Hoon et al., 2009) along with affecting basic visual processes such as visual acuity, fixation shifting, visual attention, and visual evoked potentials (Mercuri et al., 1997). Hence, there is likely significant overlap in the etiology of the motor and visual deficits seen in those with CP. Therefore, it is plausible that those with greater motor impairments may also have visual processing

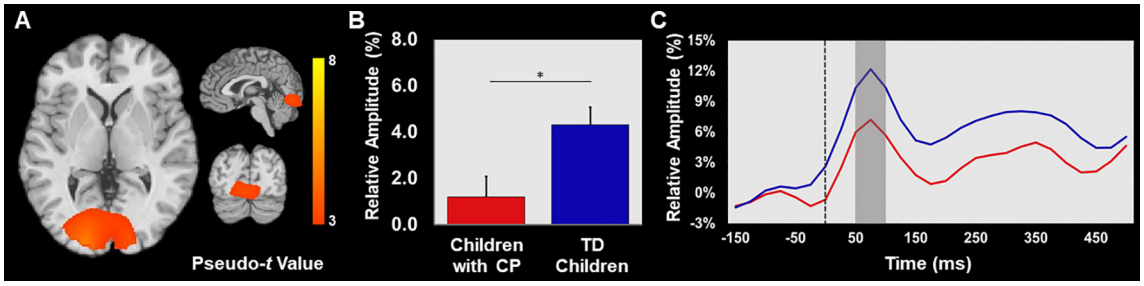

Fig. 4. Low-gamma (40 – 56 Hz) occipital responses during the 50 to100 ms time window. A) The grand-averaged beamformer image shows that the gamma increase was centered on the occipital cortices. B) Relative response values (pseudo-*t*) averaged across participants per group, with * indicating $p = 0.01$. C) The neural time course was extracted from the peak voxel of each hemisphere, and then averaged across hemispheres for each group. The time series for the group with CP are plotted in red, while the TD group are plotted in blue. Time (ms) is denoted on the *x*-axis with relative amplitude (%) shown on the *y*-axis. The visual stimulus was presented at 0 ms (dotted line), and the time–frequency window imaged is shown in the grayed area. The TD group had consistently stronger neural activity when compared with the group with CP. (For interpretation of the references to color in this figure legend, the reader is referred to the web version of this article.)

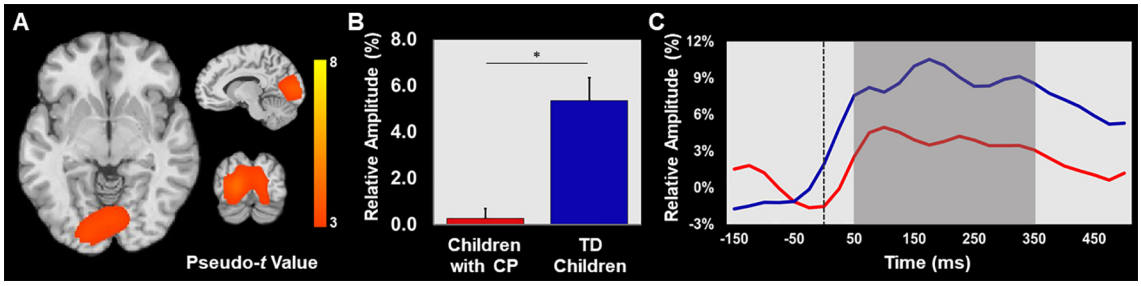

Fig. 5. High-gamma (60 – 72 Hz) occipital responses during the 50 to 350 ms time window. A) The grand-averaged beamformer image shows that the induced change in high-gamma oscillations was centered on the occipital cortices. B) Relative response values (pseudo-*t*) averaged across participants per group, with * indicating $p = 0.01$C). The neural time course was extracted from the peak voxel of each hemisphere, and then averaged across hemispheres for each group. The time series of the children with CP are plotted in red, while the TD children are plotted in blue. Time (ms) is denoted on the *x*-axis with relative amplitude (%) shown on the *y*-axis. The visual stimulus was presented at 0 ms (dotted line), and the time–frequency window imaged is shown in the grayed area. The TD group had consistently stronger neural activity when compared to the group with CP. (For interpretation of the references to color in this figure legend, the reader is referred to the web version of this article.)

deficits that synergistically affect the fidelity of their motor actions. Historically, the motor impairments in these children have been primarily seen as resulting from a musculoskeletal origin. This perception might not be completely accurate, as they might just as likely be related to perceptual processing of the environmental constraints.

Before closing, several possible limitations should be considered. While the experimental paradigm used in this investigation allowed us to explore the visual processing of contrast stimuli in children with CP, we were limited in our abilities to probe higher-level neural processes. Secondarily, our experimental data does not provide a full clinical picture of the visual disturbances in the participants, as a detailed neuro-ophthalmological evaluation was not performed. That being said, it should be recognized that the MEG assessments used here do provide a reliable and unbiased measure of visual cortical function in children with CP since they do not rely on self-report. It is also important to note that all of our participants with CP had the spastic subtype and caution should be made when expanding these results to children with non-spastic CP. Finally, we were unable to evaluate if there is a possible connection between the structural aberrations seen in children with CP and the strength of the occipital oscillations. It is possible that specific brain maldevelopments and/or white/grey matter injuries may moderate the strength of the occipital cortical oscillations.

5. Conclusion

Our experimental outcomes suggest that specific neurophysiological processes may be abnormal in the visual processing network of children with CP. Overall, our results showed deficient cortical activity serving visual processing, including weaker alpha–beta and gamma neural oscillations following high-contrast visual stimuli. Identifying deficiencies in specific neural processes may provide a target for intervention and an unbiased neurophysiological marker for evaluation. We foresee that therapeutic strategies that enhance lower-level visual processes may have cascading beneficial effects on higher-level visual-perceptual processes.

CRediT authorship contribution statement

Jacy R. VerMaas: Writing - original draft, Formal analysis, Investigation, Writing - review & editing. **Christine M. Embury:** Formal analysis, Investigation, Writing - review & editing. **Rashelle M. Hoffman:** Investigation, Writing - review & editing. **Michael P. Trevarrow:** Investigation, Writing - review & editing. **Tony W. Wilson:** Conceptualization, Methodology, Formal analysis, Supervision, Funding acquisition, Investigation, Writing - review & editing. **Max J. Kurz:** Conceptualization, Methodology, Formal analysis, Supervision, Funding acquisition, Investigation, Writing - review & editing.

Acknowledgements

This work was partially supported by grants from the National Institutes of Health (5R01HD086245; 1R01HD101833; 1P20GM130447).

References

Adjamian, P., Holliday, I.E., Barnes, G.R., Hillebrand, A., Hadjipapas, A., Singh, K.D., 2004. Induced visual illusions and gamma oscillations in human primary visual cortex. Eur. J. Neurosci. 20 (2), 587–592. https://doi.org/10.1111/j.1460-9568.2004.03495.x.

Bastos, M., Vezoli, J., Kennedy, H., Fries, P., Bastos, M., Vezoli, J., … Oostenveld, R. (2015). Visual Areas Exert Feedforward and Feedback Influences through Distinct Frequency Channels Article Visual Areas Exert Feedforward and Feedback Influences through Distinct Frequency Channels, 390–401. https://doi.org/10.1016/j.neuron.2014.12.018.

Braddick, O., Atkinson, J., 2011. Development of human visual function. Vision Res. 51 (13), 1588–1609. https://doi.org/10.1016/j.visres.2011.02.018.

Cheyne, D., Bakhtazad, L., Gaetz, W., 2006. Spatiotemporal mapping of cortical activity accompanying voluntary movements using an event-related beamforming approach. Hum. Brain Mapp. 27 (3), 213–229. https://doi.org/10.1002/hbm.20178.

Chokron, S., Dutton, G.N., 2016. Impact of cerebral visual impairments on motor skills: Implications for developmental coordination disorders. Front. Psychol. https://doi.org/10.3389/fpsyg.2016.01471.

da Cunha Matta, A.P., Nunes, G., Rossi, L., Lawisch, V., Dellatolas, G., Braga, L., 2008. Outpatient evaluation of vision and ocular motricity in 123 children with cerebral palsy. Dev. Neurorehabilit. 11 (2), 159–165. https://doi.org/10.1080/17518420701783622.

Deramore Denver, B., Froude, E., Rosenbaum, P., Wilkes-Gillan, S., Imms, C., 2016. Measurement of visual ability in children with cerebral palsy: A systematic review. Develop. Med. Child Neurol. 58 (10), 1016–1029.

Dutton, G.N., McKillop, E.C.A., Saidkasimova, S., 2006. Visual problems as a result of brain damage in children. Br. J. Ophthalmol. 90, 932–933. https://doi.org/10.1136/bjo.2006.096347.

Ego, A., Lidzba, K., Brovedani, P., Belmonti, V., Gonzalez-Monge, S., Boudia, B., Cans, C., 2015. Visual-perceptual impairment in children with cerebral palsy: A systematic review. Dev. Med. Child Neurol. 57, 46–51. https://doi.org/10.1111/dmcn.12687.

Fazzi, E., Bova, S., Giovenzana, A., Signorini, S., Uggetti, C., Bianchi, P., 2009. Cognitive visual dysfunctions in preterm children with periventricular leukomalacia. Dev. Med. Child Neurol. 51 (12), 974–981. https://doi.org/10.1111/j.1469-8749.2009.03272.x.

Fazzi, E., Signorini, S.G., Bova, S.M., Piana, R.La., Ondei, P., Bertone, C., Bianchi, P.E., 2007. Spectrum of Visual Disorders in Children With Cerebral Visual Impairment. J. Child Neurol. 22 (3), 294–301. https://doi.org/10.1177/0883073807300525.

Fazzi, E., Signorini, S.G., La Piana, R., Bertone, C., Misefari, W., Galli, J., Bianchi, P.E., 2012. Neuro-ophthalmological disorders in cerebral palsy: Ophthalmological, oculomotor, and visual aspects. Dev. Med. Child Neurol. 54 (8), 730–736. https://doi.org/10.1111/j.1469-8749.2012.04324.x.

Ghate, D., Vedanarayanan, V., Kamour, A., Corbett, J.J., Kedar, S., 2016. Optic nerve morphology as marker for disease severity in cerebral palsy of perinatal origin. J. Neurol. Sci. 368, 25–31. https://doi.org/10.1016/j.jns.2016.06.029.

Gross, J., Kujala, J., Hamalainen, M., Timmermann, L., Schnitzler, A., Salmelin, R., 2001. Dynamic imaging of coherent sources: Studying neural interactions in the human brain. Proc. Natl. Acad. Sci. 98 (2), 694–699. https://doi.org/10.1073/pnas.98.2.694.

Hall, S.D., Holliday, I.E., Hillebrand, A., Singh, K.D., Furlong, P.L., Hadjipapas, A., Barnes, G.R., 2005. The missing link: Analogous human and primate cortical gamma oscillations. NeuroImage 26 (1), 13–17. https://doi.org/10.1016/j.neuroimage.2005.01.

009.
Heinrichs-Graham, E., Arpin, D.J., Wilson, T.W., 2016. Cue-related Temporal Factors Modulate Movement-related Beta Oscillatory Activity in the Human Motor Circuit. J. Cognit. Neurosci. 28 (7), 1039–1051. https://doi.org/10.1162/jocn_a_00948.
Heinrichs-Graham, E., Wilson, T.W., 2016. Is an absolute level of cortical beta suppression required for proper movement? Magnetoencephalographic evidence from healthy aging. NeuroImage 134, 514–521. https://doi.org/10.1016/j.neuroimage.2016.04.032.
Hillebrand, A., Singh, K.D., Holliday, I.E., Furlong, P.L., Barnes, G.R., 2005. A new approach to neuroimaging with magnetoencephalography. Hum. Brain Mapp. 25 (2), 199–211. https://doi.org/10.1002/hbm.20102.
Hoon, A., Stashinko, E.E., Nagae, L.M., Lin, D.D.M., Keller, J., Bastian, A.M.Y., 2009. Sensory and motor deficits in children with cerebral palsy born preterm correlate with diffusion tensor imaging abnormalities in thalamocortical pathways. Dev. Med. Child Neurol. 51 (9), 697–704. https://doi.org/10.1111/j.1469-8749.2009.03306.x.
Ikkai, A., Dandekar, S., Curtis, C.E., 2016. Lateralization in Alpha-Band Oscillations Predicts the Locus and Spatial Distribution of Attention. PLoS ONE 11 (5), e0154796. https://doi.org/10.1371/journal.pone.0154796.
Jacobson, L., Rydberg, A., Eliasson, A.C., Kits, A., Flodmark, O., 2010. Visual field function in school-aged children with spastic unilateral cerebral palsy related to different patterns of brain damage. Dev. Med. Child Neurol. https://doi.org/10.1111/j.1469-8749.2010.03650.x.
Kerkoerle, T. Van, Self, M. W., Dagnino, B., Gariel-mathis, M., & Poort, J. (2014). Alpha and gamma oscillations characterize feedback and feedforward processing in monkey visual cortex, 111(40), 14332–14341. https://doi.org/10.1073/pnas.1402773111.
Kovach, C.K., Gander, P.E., 2016. The demodulated band transform. J. Neurosci. Methods 261, 135–154. https://doi.org/10.1016/j.jneumeth.2015.12.004.
Kozeis, Nikolaos, Panos, G. D., Zafeiriou, D. I., Gottrau, P. De, De Gottrau, P., Gatzioufas, Z., … Gatzioufas, Z. (2015). Comparative Study of Refractive Errors, Strabismus, Microsaccades, and Visual Perception between Preterm and Full-Term Children with Infantile Cerebral Palsy. Journal of Child Neurology, 30(8), 972–975. https://doi.org/10.1177/0883073814549248.
Kozeis, Nikos, Anogeianaki, A., Mitova, D. T., Anogianakis, G., Mitov, T., & Klisarova, A. (2007). Visual function and visual perception in cerebral palsied children. Ophthalmic and Physiological Optics, 27(1), 44–53. https://doi.org/10.1111/j.1475-1313.2006.00413.x.
Krigolson, O.E., Cheng, D., Binsted, G., 2015. The role of visual processing in motor learning and control: Insights from electroencephalography. Vision Res. 110 (PB), 277–285. https://doi.org/10.1016/j.visres.2014.12.024.
Kujala, J., Jung, J., Bouvard, S., Lecaignard, F., Lothe, A., Bouet, R., Jerbi, K., 2015. Gamma oscillations in V1 are correlated with GABAA receptor density: A multi-modal MEG and Flumazenil-PET study. Sci. Rep. 5 (June), 1–12. https://doi.org/10.1038/srep16347.
Kurz, M.J., Proskovec, A.L., Gehringer, J.E., Heinrichs-Graham, E., Wilson, T.W., 2017. Children with cerebral palsy have altered oscillatory activity in the motor and visual cortices during a knee motor task. NeuroImage: Clinic. 15, 298–305. https://doi.org/10.1016/j.nicl.2017.05.008.
Lee, J.D., Park, H.J., Park, E.S., Oh, M.K., Park, B., Rha, D.W., Park, C. Il., 2011. Motor pathway injury in patients with periventricular leucomalacia and spastic diplegia. Brain 134 (4), 1199–1210. https://doi.org/10.1093/brain/awr021.
Lennartsson, F., Nilsson, M., Flodmark, O., Jacobson, L., 2014. Damage to the immature optic radiation causes severe reduction of the retinal nerve fiber layer, resulting in predictable visual field defects. Invest. Ophthalmol. Vis. Sci. 55 (12), 8278–8288. https://doi.org/10.1167/iovs.14-14913.
Li, W., Piëch, V., Gilbert, C.D., 2004. Perceptual learning and top-down influences in primary visual cortex. Nat. Neurosci. 7 (6), 651–657. https://doi.org/10.1038/nn1255.
Maris, E., Oostenveld, R., 2007. Nonparametric statistical testing of EEG- and MEG-data. J. Neurosci. Methods 164 (1), 177–190. https://doi.org/10.1016/j.jneumeth.2007.03.024.
Mercuri, E., Atkinson, J., Braddick, O., Anker, S., Nokes, L., Cowan, F., Dubowitz, L., 1997. Basal ganglia damage in the newborn infant as a predictor of impaired visual function. Arch. Dis. Child. 77 (2), F111–F114.
Muthukumaraswamy, S.D., Singh, K.D., 2009. Functional decoupling of BOLD and gamma-band amplitudes in human primary visual cortex. Hum. Brain Mapp. 30 (7), 2000–2007. https://doi.org/10.1002/hbm.20644.
Muthukumaraswamy, S.D., Singh, K.D., Swettenham, J.B., Jones, D.K., 2010. Visual gamma oscillations and evoked responses: Variability, repeatability and structural MRI correlates. NeuroImage 49 (4), 3349–3357. https://doi.org/10.1016/j.neuroimage.2009.11.045.
Park, H.J., Kim, C.H., Park, E.S., Park, B., Oh, S.R., Oh, M.K., Lee, J.D., 2013. Increased GABA-A receptor binding and reduced connectivity at the motor cortex in children with hemiplegic cerebral palsy: A multimodal investigation using 18F-fluoro-flumazenil PET, immunohistochemistry, and MR imaging. J. Nucl. Med. 54 (8), 1263–1269. https://doi.org/10.2967/jnumed.112.117358.
Park, M.J., Yoo, Y.J., Chung, C.Y., Hwang, J.M., 2016. Ocular findings in patients with spastic type cerebral palsy. BMC Ophthalmology 16 (1), 1–6. https://doi.org/10.1186/s12886-016-0367-1.
Pelt, S. Van, Schoffelen, J., Kennedy, H., Fries, P., Michalareas, G., Vezoli, J., Kennedy, H., 2016. Alpha-Beta and Gamma Rhythms Subserve Feedback and Feedforward Influences among Human Visual Cortical Areas Article Alpha-Beta and Gamma Rhythms Subserve Feedback and Feedforward Influences among Human Visual Cortical Areas. Neuron 89 (2), 384–397. https://doi.org/10.1016/j.neuron.2015.12.018.
Perreault, A., Habak, C., Lepore, F., Mottron, L., Bertone, A., 2015. Behavioral evidence for a functional link between low- and mid-level visual perception in the autism spectrum. Neuropsychologia 77, 380–386. https://doi.org/10.1016/j.neuropsychologia.2015.09.022.
Piech, V., Li, W., Reeke, G.N., Gilbert, C.D., 2013. Network model of top-down influences on local gain and contextual interactions in visual cortex. Proc. Natl. Acad. Sci. 110 (43), E4108–E4117. https://doi.org/10.1073/pnas.1317019110.
Pueyo, R., Junqué, C., Vendrell, P., Narberhaus, A., Segarra, D., 2009. Neuropsychologic Impairment in Bilateral Cerebral Palsy. Pediatr. Neurol. 40 (1), 19–26. https://doi.org/10.1016/j.pediatrneurol.2008.08.003.
Rosenbaum, P., Paneth, N., Leviton, A., Goldstein, M., Bax, M., Damiano, D., Jascobsson, B., 2007. A report : The definition and classification of cerebral palsy April 2006. Dev. Med. Child Neurol. 109, 8–14. https://doi.org/10.1111/j.1469-8749.2007.tb12610.x.
Salavati, M., Rameckers, E.A.A., Steenbergen, B., Van Der Schans, C., 2014. Gross motor function, functional skills and caregiver assistance in children with spastic cerebral palsy (CP) with and without cerebral visual impairment (CVI). Eur. J. Phys. 16 (3), 159–167. https://doi.org/10.3109/21679169.2014.899392.
Saleem, A.B., Lien, A.D., Krumin, M., Busse, L., Carandini, M., Harris, K.D., 2017. Subcortical Source and Modulation of the Narrowband Gamma Oscillation in Mouse Visual Report Subcortical Source and Modulation of the Narrowband Gamma Oscillation in Mouse Visual Cortex. Neuron 93, 315–322. https://doi.org/10.1016/j.neuron.2016.12.028.
Schmetz, E., Magis, D., Detraux, J.-J., Barisnikov, K., & Rousselle, L. (2018). Basic visual perceptual processes in children with typical development and cerebral palsy: The processing of surface, length, orientation, and position. Child Neuropsychol., 00(00), 1–31. https://doi.org/10.1080/09297049.2018.1441820.
Stiers, P., Vanderkelen, R., Vanneste, G., Coene, S., De Rammelaere, M., Vandenbussche, E., 2002. Visual-perceptual impairment in a random sample of children with cerebral palsy. Dev. Med. Child Neurol. 44 (6), 370–382. https://doi.org/10.1111/j.1469-8749.2002.tb00831.x.
Swettenham, J.B., Muthukumaraswamy, S.D., Singh, K.D., 2009. Spectral Properties of Induced and Evoked Gamma Oscillations in Human Early Visual Cortex to Moving and Stationary Stimuli. J. Neurophysiol. 1241–1253. https://doi.org/10.1152/jn.91044.2008.
Takesaki, N., Kikuchi, M., Yoshimura, Y., Hiraishi, H., Hasegawa, C., Kaneda, R., Minabe, Y., 2016. The Contribution of Increased Gamma Band Connectivity to Visual Non-Verbal Reasoning in Autistic Children. A MEG Study, 1–17. https://doi.org/10.1371/journal.pone.0163133.
Taulu, S., Simola, J., 2006. Spatiotemporal signal space separation method for rejecting nearby interference in MEG measurements. Phys. Med. Biol. 51 (7), 1759–1768. https://doi.org/10.1088/0031-9155/51/7/008.
Uusitalo, M.A., Ilmoniemi, R.J., 1997. Signal-space projection method for separating MEG or EEG into components. Med. Biol. Eng. Compu. 35 (2), 135–140. https://doi.org/10.1007/BF02534144.
Van Veen, B.D., van Drongelen, W., Yuchtman, M., Suzuki, A., 1997. Localization of brain electrical activity via linearly constrained minimum variance spatial filtering. IEEE Trans. Biomed. Eng. 44 (9), 867–880. https://doi.org/10.1109/10.623056.
VerMaas, J.R., Gehringer, J.E., Wilson, T.W., Kurz, M.J., 2019. Children with cerebral palsy display altered neural oscillations within the visual MT/V5 cortices. NeuroImage: Clinical 23. https://doi.org/10.1016/j.nicl.2019.101876.
Wilson, T.W., McDermott, T.J., Mills, M.S., Coolidge, N.M., Heinrichs-Graham, E., 2017. tDCS Modulates Visual Gamma Oscillations and Basal Alpha Activity in Occipital Cortices: Evidence from MEG. Cereb. Cortex 1–13. https://doi.org/10.1093/cercor/bhx055.